Bitlis Eren Üniversitesi Fen Bilimleri Dergisi
BİTLİS EREN UNIVERSITY JOURNAL OF SCIENCE
ISSN: 2147-3129/e-ISSN: 2147-3188
VOLUME: 13 NO: 3 PAGE: 659-672 YEAR: 2024
DOI:10.17798/bitlisfen.1471235

Moleculer Docking and Theoretical Analysis of the (E)-5-((Z)-4-methylbenzylidene)-2-(((E)-4-methylbenzylidene)hydrazineylidene)-3-phenylthiazolidin-4-one Molecule

Kenan GÖREN[1], Efdal ÇİMEN[2], Veysel TAHİROĞLU[3*], Ümit YILDIKO[4]

[1]*Kafkas University, Department of Chemistry, Kars, Türkiye*
[2]*Kafkas University, Kars Vocational School, Chemistry and Chemical Processing Technologies, Kars, Türkiye*
[3]*Şırnak University, Health Sciences Faculty, Nursing Department, Şırnak*
[4]*Kafkas University, Department of Bioengineering,*

(ORCID: 0000-0001-5068-1762) (ORCID: 0000-0003-2461-5870)
(ORCID: 0000-0003-3516-5561) (ORCID: 0000-0001-8627-9038)

Keywords: DFT, MEP, NBO, ADME, Molecular Docking.

Abstract

Theoretically ideal molecular structure of (E)-5-((Z)-4-methylbenzylidene)-2-(((E)-4-methylbenzylidene)hydrazineylidene)-3-phenylthiazolidin-4-one (EMPT) Gaussian 09 software was researched using. The theoretically ideal chemical structure of EMPT molecule has been examined. The B3LYP/SDD-B3LYP/6-311G bases and techniques were used to perform quantum chemical calculations. To find out how the molecule transfers charge, LUMO and HOMO analyses were done. The stability of the molecule was investigated as a function of charge dispersion and hyperconjugative interaction using NBO analysis. MEP was reported to be performed using a DFT technique. We observed the compatibility of HOMO-LUMO, MEPS, NLO, Mulliken Atomic Charges and optimized molecular geometry data in the two sets used. Molecular docking studies were performed using enzyme codes PDB: 5FGK and PDB: 5HBE to determine the binding affinity and possible fundamental interaction betwith the inhibitors and the target enzyme. Finally, in our study, ADME analysis of EMPT molecule was performed and many parameters were examined using virtual screening methods on small molecules, Molecular characteristics, cell permeability, HIA drug solubility S, medicament paralely point and polar surface area PSA are among them.

1. Introduction

Schiff bases are compounds generally represented by the formula R-CH=N-R'. In this formula, R and R' represent aryl or alkyl substituents. Schiff bases and some Schiff complexes are widely used in both synthesis and medical fields. These substances are very important due to the pharmacological effects of heterocycles [1]. Medicinal chemists utilize heterocyclic compounds with five and six members that are oxygen, sulfur, and nitrogen-containing. Diazoles or oxazole derivatives containing oxygen along with nitrogen as heteroatoms in the quintuple ring are very important due to their anti-inflammatory, antidepressant, analgesic, anti-cancer, antimicrobial, antidiabetic, and anti-obesity qualities. In other words, Schiff bases have also been studied because they are also used to form covalent organic frameworks [2]. These frameworks contain two- or three-size spongy crystal formation and utilize Schiff base interactions through covalent molecular assembly. Additionally, most Schiff bases exhibit remarkable coordination properties with metallic ions, forming corresponding complexes comprising actinide, lanthanide, transition metal, and main group elements [3]. When combined with a metal ion, its

*Corresponding author: veysel.tahiroglu@sirnak.edu.tr
Received: 20.04.2024, Accepted: 08.08.2024

characteristics are greatly enhanced. Its properties are significantly improved when coordinated with a metal ion. Schiff base ligands can be made quickly and combine with nearly all metal ions to form complexes [4]. Its antibacterial, antifungal, antioxidant, anticancer, anti-inflammatory, antimalarial, and antiviral properties have been utilized in biology. Moreover, they function as catalysts for a range of processes, such as the synthesis of bis(indomethacin) and polymerization, thionyl chloride reduction, oxidation of organic compounds, ketone reduction reaction, aldol reaction, Henry reaction, epoxidation of alkenes, and hydrosilylation of ketones. Additionally, there is evidence in the literature that it is used for the synthesis of hetero compounds or protecting groups in organic syntheses [5]. The development of contemporary computational simulation techniques has made it possible to compute orbital, optical, and structural properties with accuracy. Therefore, without conducting experimental research, it is feasible to predict the physical, chemical, and optical possessions of different nanomaterials, including molecules and alloys. The nonlinear visual (NLO) possessions of materials play a major role in signal processing, optical switches, and optical memory design in communications technology. The NLO properties of molecules arise from the movement of delocalized π-electrons around them. Increased conjugation and the addition of acceptor and donor groups to the molecule changes the NLO property [6]. Especially for such chemicals, which are difficult to examine in terms of analytical chemistry, preparation is required through data processing and statistical evaluation, optimization of experimental factors, time saving, calibration and theoretical calculations required for quantitative measurements [7]. Even in very large and complex systems, results can be obtained in a reasonable time. One of the fundamental principles of quantum chemical methods is approaches based on density functional theory (DFT) [8].

Since the DFT (B3LYP) method and 6-311G and SDD basis sets have been widely used in the literature, we preferred these methods in terms of docking interaction by making energy calculations, charge calculations and optimization of the potentially used molecule. Molecular modeling investigations of the chosen EMPT molecule compound were conducted in this work. to learn more about the compound's energy, electrical, and nonlinear optical properties, DFT investigations were conducted. Furthermore, ADME analysis was carried out to look into the compound's ADME characteristics. Ultimately, successful molecular docking done were do to ascertain whether the EMPT molecule compound would be consistent with the drug design phenomena.

2. Material and Method

First, utilizing the Gaussian 09 software, EMPT molecule was drawn in ChemBioDraw for computations with DFT [9] and then reduced using the Chem3D program technique. In a similar manner, GaussView 6.0 was opened after the sketched molecules had been transformed to 3D MOL2 files in Chem3D. The B3LYP/SDD-B3LYP/6-311G bases and techniques were used to compute the DFT research. Each calculation's results, including HOMO and LUMO analysis, geometry optimization, Mulliken atomic charge and dipole moment, and MEP analysis, have been displayed. Schrödinger's Maestro Molecular Modeling platform (version 12.5) was utilized to accomplish molecular docking, which allowed for the precise identification of the binding mechanism and connecting site of ligand-protein interactions. For the ADME test, online servers like SwissADME (http://www.swissadme.ch/index.php) were utilized. The protein data bank's PDB: 5FGK and PDB: 5HBE enzyme codes were used for the docking analysis. The Discovery Studio 2016 client helped to conceptualize the molecular docking study.

3. Results and Discussion

3.1. Structure details and analysis

Using the GaussView 6.0 molecular imaging program, the approximate three-dimensional geometry of the EMPT molecule compound was drawn and the atomic positions were determined. All not practical compitation were made utilize the Gaussian 09W package aplication [9]. The structure of the examined molecule obtained from the literature [1] and the theoretically calculated geometric structure utilize the B3LYP/SDD-B3LYP/6-311G basis set and approaches are shown with atoms. B3LYP theory was used, which includes the Lee-Yang and Parr correlation functional [8]. Becke's hybrid energy functional approach with three parameters, and DFT coded in the Gaussian 09W program. The basis set used in the calculations is 6-311G(d,p); This set includes diffuse functions and polarized functions, which are added to model the situation where the electron density in excited ionic molecules is more dispersed than in the ground state of the molecule. To eliminate the polarization effect (when atoms are brought closer together, the electronic density is distorted by the influence of other nuclei). Bond lengths (Å) and bond angles (Å) for the

molecule are listed in Table 1 using approximations and the B3LYP/SDD-B3LYP/6-311G basis set.

Improved performance based on comparison of the EMPT molecule was investigated. The bond lengths and bond angles in the phenyl rings are within the standart reach. For the oxygen atom in the two phenyl rings, the C–O Nexus range for B3LYP are 1.20 Å and the C–C bond gap are 1.349–1.489 Å. The aromatic content in the C–H ring is 1.083–1.087 Å. Each angle C-C-C is 117° and its slope is 120.5°. N-C-O 123°, C-C-H 120°, C-N-C 118°, C-S-C 91°, N-N-C 112°, C-N-C 118°, H-C-H 107° and C-O bond distances 1.21 Å, C-C bond distances 1.352-1.484 Å for B3LYP/6-311G. The aromatic content in the C–H ring is 1.086–1.089 Å. Each angle C-C-C is 117° and its slope is 120°. N-C-O is 123°, C-C-H is 120°, C-N-C is 118°, C-S-C is 92°, N-N-C is 111°, H-C-H is 107°. When we looked at a similar molecule in the literature, we observed similar bond length values when compared with experimental data [10].

Table 1. Theoretically determined some bond lengths (Å) and angles (°) of the EMPT molecule

Bond Lengths	**B3LYP/ SDD**	**B3LYP/ 6-311G**	**Bond Lengths**	**B3LYP/ SDD**	**B3LYP/ 6-311G**
C1-C2	1.39389	1.39427	**C12-H36**	1.08709	1.08949
C3-C4	1.39034	1.39145	**C14-H37**	1.08480	1.08712
C5-C6	1.39162	1.39163	**C22-H41**	1.08534	1.08761
C8-C9	1.48792	1.48474	**C8-N7**	1.41227	1.43783
C12-C13	1.45212	1.44997	**C11-N7**	1.39081	1.38840
C9-C12	1.34955	1.35205	**C30-N20**	1.28462	1.28847
C21-C30	1.45907	1.45625	**C8-O29**	1.20844	1.21363
Bond Angles	**B3LYP/ SDD**	**B3LYP/ 6-311G**	**Bond Angles**	**B3LYP/ SDD**	**B3LYP/ 6-311G**
C1-C2-C3	120.13201	120.17183	**C1-C2-H32**	120.17654	120.18659
C4-C5-C6	119.47092	119.41537	**H45-C27-H46**	107.88369	107.93864
C8-C9-C12	119.51263	119.25575	**N7-C8-O29**	123.29208	123.41517
C12-C13-C14	117.86380	117.80464	**C9-S10-C11**	91.10198	92.16928
C4-N7-C8	118.10449	118.05547	**N19-N20-C30**	112.23423	111.80088
Planar Bond Angles	**B3LYP/ SDD**	**B3LYP/ 6-311G**	**Planar Bond Angles**	**B3LYP/ SDD**	**B3LYP/ 6-311G**
C1-C2-C3-C4	-0.50573	-0.36664	**C11-N19-N20-C30**	179.93208	177.64062
C8-C9-C12-C13	-179.89223	-179.57650	**C4-N7-C11-S10**	179.58625	175.81861
C3-C4-N7-C11	92.80774	10218577	**N7-C8-C9-C12**	179.94703	179.64806
C4-N7-C8-O29	0.31301	3.22207	**O29-C8-C9-12**	-0.02363	-0.066774

3.2. Mulliken atomic charges

Unlike electron density, atomic charges cannot be calculated precisely using quantum mechanics. So there is some degree of randomness in every method developed to calculate this quantity. Despite some disadvantages, the Mulliken load distribution method is widely used [11]. The Mulliken charge distribution method is based on distributing wave functions between atoms and dividing equally the regions where two orbitals overlap. However, this distribution does not accurately represent the electronegativity of each element [12]. In some extreme cases, it may result in an orbital with a negative electron population or describe an orbital with more than two electrons. These are based heavily on the chosen base. Therefore some qualitative estimates are made using Mulliken loadings instead [13].

In this study, Mulliken load values calculated with the Gaussian 09W program as a result of any optimization were evaluated for the purpose of calculating atomic loads. Table 2 shows the gas phase studied using the B3LYP/SDD-B3LYP/6-311G basis set and approximations. It was determined that the electronegative atoms (N7, N11, N19, N20 and O29) in the molecule had negative charge values. The calculated charge values of these atoms are -0.497, -0.253, -0.250 and -0.323 (a.u.). Figure 1 shows Structure Optimization using the DFT/B3LYP/6-311G basis set and approaches.

Table 2. Mulliken atomic charges of the EMPT molecule

ATOMS	B3LYP/ SDD	B3LYP/ 6-311G	ATOMS	B3LYP/ SDD	B3LYP/ 6-311G
C1	-0.093	-0.113	**O29**	-0.323	-0.485
C2	-0.101	-0.142	**N7**	-0.497	-0.641
C3	-0.008	-0.075	**N19**	-0.253	-0.355
C4	0.119	0.235	**N20**	-0.250	-0.325
C5	-0.008	-0.072	**S10**	0.252	0.299
C6	-0.101	-0.139	**H31**	0.097	0.124
C8	0.525	0.657	**H32**	0.099	0.129
C9	-0.419	-0.261	**H33**	0.090	0.137
C12	0.032	-0.150	**H34**	0.090	0.135
C13	-0.071	0.095	**H35**	0.099	0.129
C14	-0.059	-0.147	**H36**	0.125	0.165
C15	-0.075	-0.152	**H37**	0.093	0.129
C16	-0.091	0.101	**H38**	0.089	0.121
C17	-0.078	-0.155	**H39**	0.087	0.122
C18	-0.059	-0.141	**H40**	0.104	0.132
C21	-0.165	0.047	**H41**	0.089	0.122
C22	-0.052	-0.145	**H42**	0.085	0.116
C23	-0.076	-0.158	**H43**	0.083	0.116
C24	-0.088	0.103	**H44**	0.141	0.157
C25	-0.099	-0.154	**H45**	0.107	0.138
C26	-0.020	-0.123	**H46**	0.125	0.148
C27	-0.256	-0.448	**H47**	0.125	0.152
C28	-0.257	-0.448	**H48**	0.117	0.144

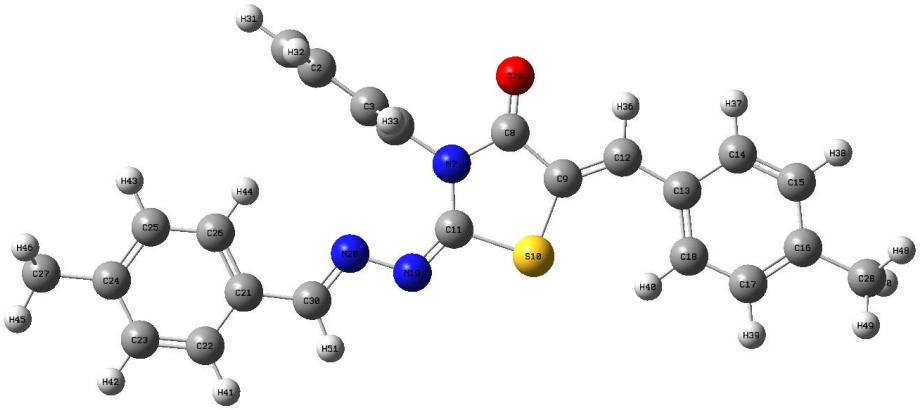

Figure 1. EMPT molecule with DFT/B3LYP/6-311G basis Structure Optimization

3.3. HOMO and LUMO analysis

Molecular orbital theory states that atoms combine to form molecules. When the atomic orbitals that make up the molecules approach each other by the required bond distance, they combine to create the molecule's orbitals. These orbitals can be thought of as places in the molecule where there is a maximum chance of finding an electron [14]. The lowest energy of unoccupied molecular orbitals (ELUMO) and the highest energy of occupied molecular orbitals (EHOMO) are found in the fundamental orbitals involved in chemical reactions [15]. The skill of a molecule to make a donation of electrons (π donor) is known as HOMO energy and the skill of a molecule to accept electrons (π acceptor) is known as LUMO energy.

The minimal unoccupied molecular orbital (LUMO) and the maximum occupied molecular

orbital (HOMO) are two crucial molecular orbitals. The bioactivity of a chemical is represented by its eigenvalues and hole energies for LUMO and HOMO. Shorter frontier orbital spaces cause a chemical to be more polarized, have less kinetic stability, and be more reactive toward chemicals [16]. Since the HOMO is the outer orbital that carries electrons and attempts to act as an electron donor, its energy has a direct impact on the ionization potential. However, LUMO has the potential to absorb electrons and its energy is involved to the electron proximity. The HOMO and LUMO chemicals' eigenvectors and energy gaps show the molecule's biological activity [17]. Figures 2 and 3 display the EMPT molecule's HOMO and LUMO energies, which were deternined using the B3LYP/SDD-B3LYP/6-311G basis set and methodologies. Two significant chemical orbitals for HOMO and LUMO energies were investigated, as shown in Figures 2 and 3. Table 3 displays the quantum chemical factor (in eV) determined for the nominal energy conformation of the EMPT molecule utilizing the DFT/B3LYP/6-311G and DFT/B3LYP/SDD techniques. When we examine two important chemical orbitals for HOMO and LUMO energies in Figures 2 and 3, the HOMO and LUMO electron clouds are completely located throughout the ligand, except for the aromatic ring (C1, C2, C3, C4, C5, C6). In addition, LUMO+1 electron clouds are completely localized throughout the ligand, except for the (C1, C2, C3, C4, C5, C6) aromatic ring, while HOMO-1 has been localized on the (C1, C2, C3, C4, C5, C6) aromatic ring and (E)-3-methyl-2-(methylimino)thiazolidin-4-one. We observed that the localized regions were the same in both sets. The localized regions are the same in both sets, indicating that boundary molecular orbitals have important roles in chemical reactivity and stability.

The orbital energies of LUMO and HOMO can be used in the following formulas to calculate the electron proximity and ionization energy: A=−ELUMO, I=−EHOMO, (μ=−(I+A)/2) and η=(I−A)/2. An electrophilic system can store more electrons and resist the transfer of electrons to the environment than a non-electrophilic system [18]. It is a more accurate measure of total chemical reactivity because it contains information about both electron transfer (potential chemical) and durability (hardness). Chemical species are the affinity and ionization potential of electrons; Chemical potential and hardness (A) are calculated using the formulas=(IA)/2 and =(I+A)/2, respectively [19].
The stable and negative chemical potential resulting from the negativity of this complex prevents the spontaneous dissolution of the components forming the title compound. An electron nebula's resistance to degradation caused by small perturbations during chemical processing is what gives it its hardness. Although it cannot be observed physically, both chemistry and physics make use of the notion of hardness. In contrast to soft systems, which can be highly and significantly polarized, hard systems are typically much smaller and less polarized.

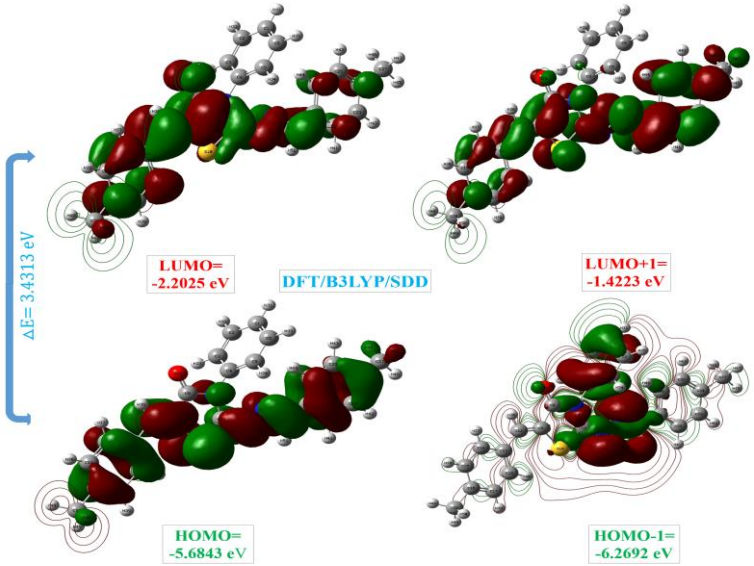

Figure 2. Boundary molecular orbitals of the EMPT molecule as per the DFT/B3LYP/SDD phase

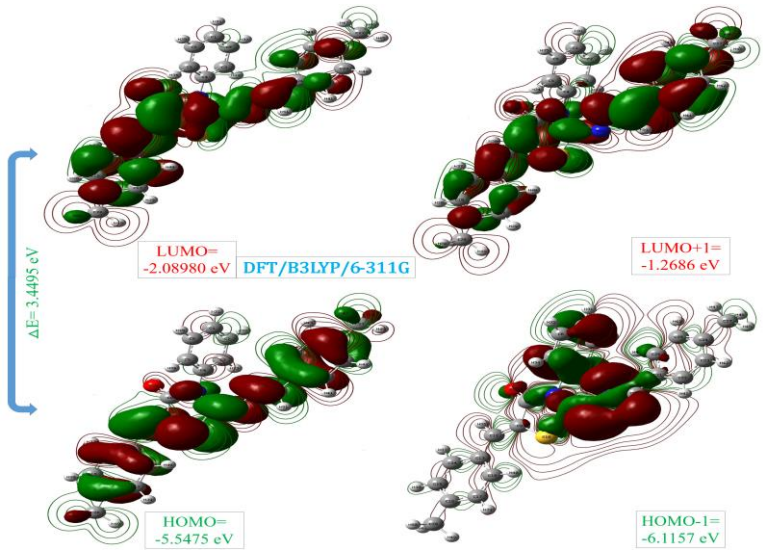

Figure 3. Boundary molecular orbitals of the EMPT molecule as per the DFT/B3LYP/6-311G level

Table 3. Quantum chemical parameters (in eV) of the EMPT molecule were calculated using the DFT/B3LYP/SDD-DFT/B3LYP/6-311G methods, leading to low energy compatibilities

Molecules Energy		DFT/B3LYP SDD	DFT/B3LYP 6-311G
E_{LUMO}		-2.2025	-2.0980
E_{HOMO}		-5.6849	-5.5475
E_{LUMO+1}		-1.4223	-1.2686
E_{HOMO-1}		-6.2692	-6.1157
Energy Gap	$(\Delta E)\|E_{HOMO}-E_{LUMO}/$	3.4824	3.4495
Ionization Potential	$(I=-E_{HOMO})$	5.6849	5.5475
Electron Affinity	$(A=-E_{LUMO})$	2.2025	2.0980
Chemical hardness	$(\eta=(I-A)/2)$	1.7412	1.7248
Chemical softness	$(s=1/2\eta)$	0.8706	0.8624
Chemical Potential	$(\mu=-(I+A)/2)$	-3.9437	-3.8228
Electronegativity	$(\chi=(1+A)/2)$	1. 6013	1.549
Electrophilicity index	$(\omega=\mu^2/2\eta)$	13.5402	12.6029

3.4. Molecular electrostatic potential (MEP)

The predicted atomic charges are defined to calculate the atomic charges. The electrostatic potential (ESP) is determined by defining multiple points surrounding the molecule under study, provided that the atomic charges obtained from the least squares method correspond to the electrostatic potential [20]. These charges may vary slightly because the electrostatic potential calculation is based on estimating the locations of spatial points. Electronegativity and partial charges are related to ESP [21]. Together with the ESP potential surface, Figure 4 displays Molecular electrostatic potential field (MEP) mapped [22].

MEP can be used to identify hydrogen bond interactions in addition to electrophilic and nucleophilic activities. The relationship is with electron density (ED). The electrostatic potential V(r) is a useful tool for molecular characterization research procedures, such as studying the relationships between medications and receptors or between substrates and enzymes. Because these two types initially perceive each other through the lens of their prospective [23]. The electrophilic and nucleophilic moieties of the studied complex were divine utilize B3LYP/SDD-B3LYP/6-311G basis set using MEP in the optimal geometry. As shown in Figure 4, negative (yellow or red) regions of the MEP indicate electrophilic reaction, whereas favorable (blue) regions represent nucleophilic reactivity. As we expected, the negative regions were localized to the oxygen on the thiazolidine ring.

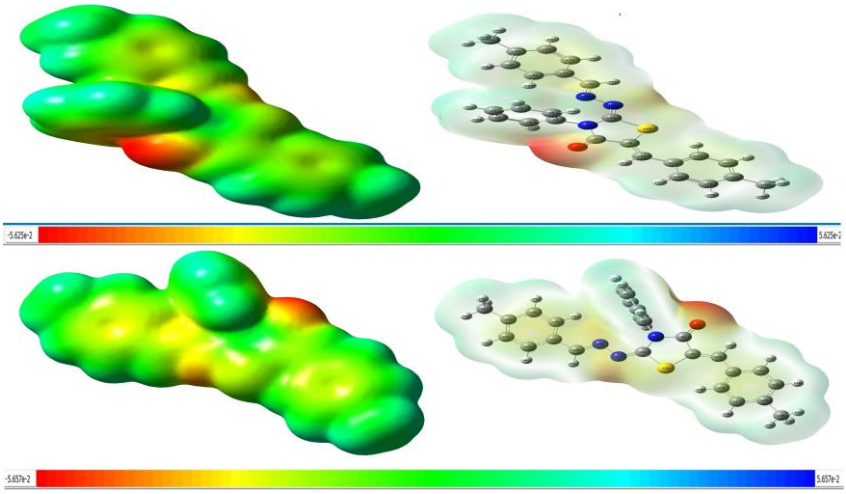

Figure 4. Molecular electrostatic potential field of EMPT molecule utilising B3LYP/SDD-B3LYP/6-311G methods and basis.

3.5. Non-Linear optical properties (NLO)

Polarizability (α) and hyperpolarizability (β) values are used to computationally predict nonlinear optical properties (NLO). Optical properties in organic matter-based materials are defined by their polarizability [24]. The performance of a material's nonlinear optical properties is affected by its hyperpolarizability. A molecule needs to have a small HOMO-LUMO energy difference, a high dipole moment, polarizability, and hyperpolarizability in order to exhibit the NLO property [25]. Hyperpolarization (β), polarization (α), and electric dipole moment (μ) of EMPT molecule were measured using NLO activity, B3LYP/SDD(d,p) and B3LYP/6-311G method and basis set. Calculated NLO values are shown in Table 4.

Equations 1–4 gave the average polarizability (α), static dipole moment (μ), and total first static hyperpolarizability (β) values for the x, y, and z components. DFT/B3LYP/6-311G and DFT/B3LYP/SDD approaches gave total values of 3.47x10-30 esu and 3.54x10-30 esu for EMPT molecule, respectively.

$$\mu = (\mu_x^2 + \mu_z^2)^{1/2} \quad (1)$$

$$\alpha = 2^{-1/2}\left[\left(\alpha_{xx} - \alpha_{yy}\right)^2 + \left(\alpha_{yy} - \alpha_{zz}\right)^2 + (\alpha_{zz} - \alpha_{xx})^2 + 6{\alpha_{xx}}^2\right]^{1/2} \quad (2)$$

$$\beta_{Total} = (\beta^2 x + \beta^2 y + \beta^2 z)^{1/2} \quad (3)$$

$$= [(\beta xxx + \beta xyy + \beta xzz)^2 + (\beta yyy + \beta yxx + \beta yzz)^2 + (\beta zzz + \beta zxx + \beta zyy)^2]^{\frac{1}{2}} \quad (4)$$

Table 4. The dipole moments (Debye), polarizability (au), components, and total value of EMPT molecule are computed using the SDD and 6-311G basis s using the DFT/B3LYP technique

Parameters	B3LYP/ SDD	B3LYP/ 6-311G	Parameters	B3LYP/ SDD	B3LYP/ 6-311G
μ x	0.4280	0.3405	**β xxx**	-86.9694	-90.0332
μ y	-0.9119	-0.8372	**β yyy**	-47.3193	-44.5391
μ z	0.0580	0.2335	**β zzz**	0.9476	2.6570
μ (D)	1.0091	0.9335	**β xyy**	35.0618	34.4839
α xx	-128.8197	-123.5322	**β xxy**	-32.3496	-33.6734
α yy	-177.9241	-173.1954	**β xxz**	3.1931	3.2352
α zz	-182.3465	-178.3604	**β xzz**	13.1104	13.5166
α xy	8.7467	9.0193	**β yzz**	24.4836	23.6049
α xz	-0.3724	0.0065	**β yyz**	-0.3900	-0.6371
α yz	-0.1230	-1.2630	**β xyz**	0.7795	-1.1306
α (au)	-184.972	-184.7400	**β (esu)**	$3.47x10^{-30}$	$3.54x10^{-30}$

3.6. NBO Analysis

To better understand the intermolecular interactions in EMPT molecule, NBO analysis was performed on the optimized structures [26]. The Gaussian 09W program package was used to make the NBO analysis. The percentages of individual bond electrons for σ and π bonds in various bonds using DFT(B3LYP) methods and the changes in the percentages of electrons in s, p, and d orbitals in each atom are shown in Table 5 comparisons. Hybridizations that occur to form bonds on atoms are also obtained from this pointIn this instance, π bonds by definition have to be made up of the p atomic orbitals of the C, O, and N atoms. Research has demonstrated how much the s orbital helps with hybridization at the C atom. Table 5 shows the changes in the percentages of electrons in s, p, and d orbitals in each atom, as well as the percentages of individual bond electrons and bonds in different bonds. A quadratic expression is used for EMPT molecule. Fock marix was used to estimate the relationship between the receiver (j) and the transmitter (i). The compensatory value associated with delocalization is estimated to be as in Equation 5 for each giver (i) and recipient (j) [27].

$$E(2) = \Delta Eij = qi\frac{(Fi,j)^{2}}{(\mathcal{E}i - \mathcal{E}j)} \quad (5)$$

The NBO element of the Fock matrix is F(i,j), the diagonal elements are i and j, and the donor orbital occupancy is qi. An increase in stabilization energy increases the probability of electrons moving to acceptor orbitals. For a few chosen donors and acceptors, Table 5 displays the electron volume, E(2), E(j)-E(i), and f(i,j) values along with the results of the NBO calculations. The relationship between electron delocalization from bonding (BD) to antibonding (BD*) orbitals, filled and unfilled NBO-type Lewis orbitals, and stabilization energy E(2) is characterized by NBO analysis. The interactions between bond (σ/π) and anti-bond (σ*/π*) also have a significant impact on structural stability. π(C16-C17) /π*(C13-C18) interaction has the maximum E value with 22. kcal/mol. (2), followed by π(C23-C24)/π*(C21-C22) interaction with 22.40 kcal/mol.

Table 5. Selected NBO results of EMPT molecule are computed using the DFT/B3LYP technique and the SDD basis

NBO(i)	Type	Occupancies	NBO(j)	Type	Occupancies	E(2)[a] (Kcal/mol)	E (j)-E(i)[b] (a.u.)	F (i, j)[c] (a.u)
C1-C6	π	1.66189	**C4-C5**	π *	1.66443	21.04	0.29	0.069
C1-H31	σ	1.97929	**C2-C3**	σ *	1.97429	3.88	1.10	0.058
C2-C3	σ	1.97429	**C4-N7**	σ*	1.97588	4.87	1.07	0.065
C3-C4	σ	1.97183	**C4-C5**	σ *	1.97182	4.67	1.28	0.069
C4-C5	π	1.66443	**C2-C3**	π*	1.97429	20.82	0.29	0.070
C5-C6	σ	1.97429	**C4-N7**	σ *	1.97588	4.87	1.07	0.065
C6-H35	σ	1.97932	**C1-C2**	σ*	1.97882	3.85	1.09	0.058
C8-C9	σ	1.96956	**C12-C13**	σ*	1.97275	5.96	1.18	0.068
C8-O29	π	1.98122	**C9-C12**	π*	1.84583	3.33	0.41	0.035
C9-C12	π	1.84583	**C8-O29**	π*	1.98122	20.07	0.30	0.072
S10-C11	σ	1.96241	**N19-N20**	σ *	1.96946	6.39	1.02	0.072
C11-N19	π	1.90607	**N20-C30**	π *	1.89638	11.41	0.37	0.059
C12-C13	σ	1.97275	**C9-C12**	σ*	1.97857	4.97	1.31	0.072
C12-H36	σ	1.95997	**C9-S10**	σ *	1.97510	1.15	0.70	0.079
C13-C18	π	1.61305	**C14-C15**	π*	1.67863	19.42	0.28	0.068
C14-C15	π	1.67863	**C16-C17**	π *	1.62397	21.37	0.29	0.071
C14-H37	σ	1.97943	**C13-C18**	σ*	1.97161	4.34	1.08	0.061
C15-H38	σ	1.97891	**C16-C17**	σ *	1.97352	4.36	1.09	0.062
C16-C17	π	1.62397	**C13-C18**	π*	1.61305	22.96	0.28	0.072
C17-H39	σ	1.97915	**C15-C16**	σ*	1.97335	4.39	1.09	0.062
N19-N20	σ	1.96946	**S10-C11**	σ*	1.96241	5.46	0.96	0.065
N20-C30	π	1.89638	**C11-N19**	π *	1.90607	13.58	0.32	0.062

C21-C22	π	1.63648	**N20-C30**	π *	1.89638	20.18	0.27	0.069
C22-H41	σ	1.97942	**C21-C26**	σ*	1.97115	4.46	1.08	0.062
C23-C24	π	1.64733	**C21-C22**	π *	1.62648	22.40	0.28	0.072
C25-C26	π	1.68248	**C21-C22**	π *	1.63648	18.52	0.28	0.066
C28-H50	σ	1.97391	**C16-C17**	σ *	1.62397	4.65	0.54	0.049

3.7. Molecular docking studies

The process of observing and analyzing interactions between a ligand and a protein sensor is called molecular docking [28]. A computer technique called "molecular docking" attempts to predict the noncovalent interaction between a small molecule (ligands) and a macromolecule (receptor). Automated docking has been extensively utilized in molecular design and structure/function analysis to forecast the configurations of bimolecular complexes [29]. Docking small molecule compounds into receptor binding sites and assessing the complex's binding affinity are two steps in the structure-based drug design process. The complexes of proteins of these enzymes have been discovered by investigating the online resource RSCB protein database for 5FGK and PDB: 5HBE. Enzyme codes PDB: 5FGK and PDB: 5HBE were used in molecular docking studies to ascertain the inhibitors' binding affinities and potential interactions with the target enzyme. The 5FGK and 5HBE proteins encoded by this gene are members of the cyclin-dependent protein kinase (CDK) family. CDK8 and cyclin C are associated with the mediator complex and regulate transcription by various mechanisms. CDK8 binds and/or phosphorylates a variety of transcription factors, which can have an activating or inhibitory effect on transcription factor function. CDK8 phosphorylates the Notch intracellular domain SREBP and STAT1 S727. CDK8 also inhibits transcriptional activation by affecting turnover of subunits in the tail module of the mediator complex. The molecular docking scores of PDB: 5FGK and PDB: 5HBE enzymes are shown in Table 6.

Table 6. Docking score of EMPT molecule for PDB: 5FGK, PDB: 5HBE enzyme and control

Compound	**Docking Score (**cal/mol)			
	PDB: 5FGK	Control 5FGK	PDB: 5HBE	Control 5HBE
EMPT Molecule	-7.10	-9.72	-6.11	-8.20

As a result of the docking study of EMPT molecule, Figure 5 shows their 2D and shows its interaction in 3D modes. As a result, in Table 6, the shift score with molecule (the (E)-5-((Z)-4-methylbenzylidene)-2-(((E)-4-methylbenzylidene)hydrazineylidene)-3-phenylthiazolidin-4-one)-PDB:5FGK was determined as -7.10 cal/mol and the shift score with PDB:5HBE was determined as -6.11 cal/mol. Here is the binding mechanism, Thiazolidin-4-one ARG-356 (4.47 Å), p-xylene pi-pi form HIS-106 (7.04 Å), benzene pi-alkyl LEU-158 (6.21 Å), VAL-35 (5.56 Å), ALA-50 (5.35 Å), benzene alkyl ALA-50 (5.02 Å), ILE-79 (4.34 Å), PHE-97 (3.80 Å), for van der Waals structures, other interactions with GLU-357, TYR- 99, ALA-155, ALA-172, ASP-173 are shown in Figure 6. Figure 6 shows a 3D view of the SAS surface on the receptor.

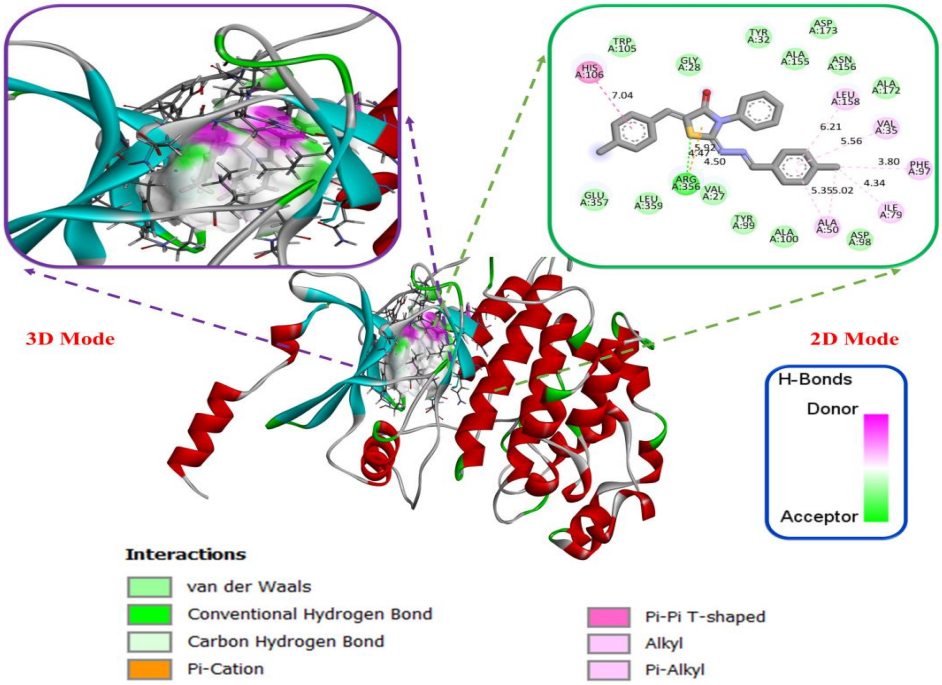

Figure 6. Ligand-5FGK mode of interaction with enzymes; 3D view of the donor/acceptor surface of hydrogen bonds on the receptor and 2D view of ligand enzyme interactions

As a result of the EMPT molecule 5HBE placement study, it is as shown in the 3D and 2D views in Figure 6. With PDB: 5HBE, the shift score was determined as -6.11 cal/mol. The binding mechanism is here, Thiazolidin-4-one TYR-32 (6.1 Å), benzene pi-alkyl LEU-158 (6.09 Å), VAL-35 (5.06 Å), ALA-100 (5.06 Å), benzene alkyl ALA-50 (4.59 Å), ILE-79 (4.61 Å), PHE-97 (5.48 Å), for van der Waals structures, TRP-105, TYR-32, ALA Other interactions with -155, ALA-172, ASP-173, ARG-356, VAL-27, HIS-106 are shown in Figure 7.

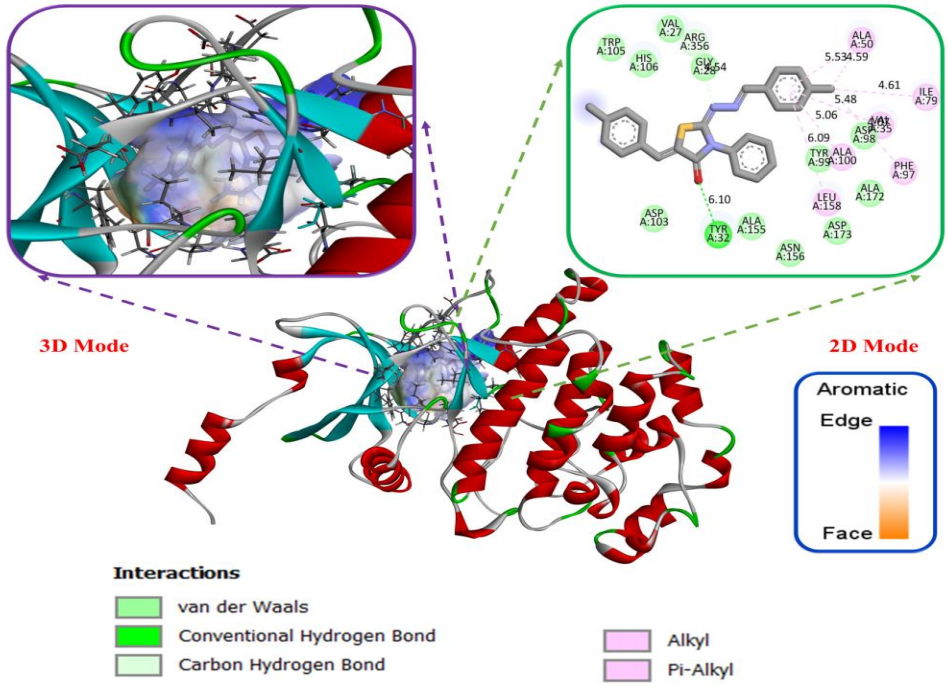

Figure 7. Molecule-5HBE mode of interaction with enzymes; a) 3D view of the donor/acceptor surface of aromatic bonds on the receptor b) 2D view of ligand enzyme interactions

Figure 8. Control Ligand-5FGK 2D Mode and control Ligand-5HBE 2D Mode view have been shown. When we look at the docking scores in Table 6, the binding scores for both proteins were found to be close to the binding scores of the natural ligand. The compatibility difference was created during the optimization and creation of the logbox. However, binding in the pocket created here was achieved in sufficient amounts for enzyme inhibition.

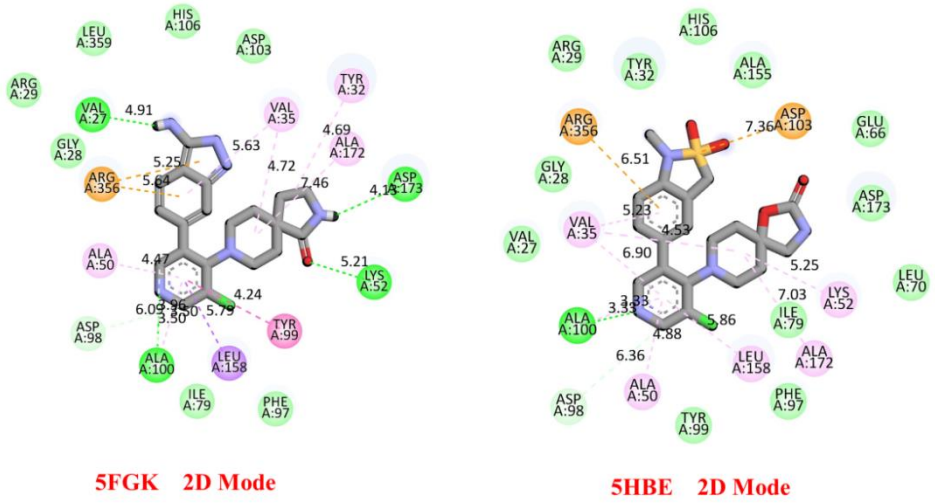

Figure 8. Control Ligand-5FGK 2D Mode and control Ligand-5HBE 2D Mode view

3.8. ADME analysis

Currently, the most promising compounds are selected through ADME studies in drug production in order to reduce the possibility of drug attrition in the final stage. These studies can be used as preliminary data to determine the balance between pharmacodynamic and pharmacokinetic properties [29]. Virtual screening methods have been applied to small molecules to investigate a variety of factors, like molecular quality, drug ability S, cell permeability, HIA, polar plane area PSA, and drug resemblance mark [30]. Bileşiklerin ilaca benzer bir yapıya sahip olup olmadığını ve canlı organizmalardaki aktivitesini tespit edebilmek için Lipinskinin beş kriteri, Veber ve Egan kriterleri gibi bazı kriterler vardır. Bu çalışmada başlıkta adı geçen bileşiğin ilaç benzerlik özellikleri Lipinski kriterleri kullanılarak araştırılmıştır. Lipinski's rule of five is a method of analysis to calculate the drug similarity of the compound and also to determine whether a chemical compound with a certain pharmacological or biological activity can be used as an active and orally active drug in humans. According to the rule of five determined by Lipinski as a result of his studies, a molecule must meet these conditions (Molecular Weight (MW) ≤500 g/mol, lipophilicity coefficient LogP≤5, hydrogen bond donor ≤5, hydrogen bond acceptor ≤10, molar break values 4-130) in order to be a drug candidate [31]. A pharmaceutical product that is currently on the market that is chosen based on Lipinski's rule of five should have a molecular weight of no more than 500 and a logP of no more than 5, along with fewer than 10 hydrogen bond acceptors and fewer than 5 hydrogen bond donors [32]. Based on the data presented in Table 7, our compound complied with Lipinski's guidelines and produced satisfactory results for adme analysis.

Table 7. Physicochemical and lipophilicity of EMPT molecule

Code EMPT Molecule	Lipophilicity consensus log P	Physico-chemical properties								
		MW[a] g/mol	Heavy Atoms	Aromatic heavy atoms	Rot. bond	H-acceptor bond	H-donor bond	MR[b]	TPSA[c] (A^2)	% ABS[d]
	3.46	411.52	30	18	4	3	0	130.28	70.33	84.73

[a]**MW**, molecular weight; [c]**TPSA**, topological polar surface area; [b]**MR**, molar refractivity; [d]**ABS%:** absorption percent $ABS\% = 109 - [0.345 \times TPSA]$.

4. Conclusion

Important geometric data, including bond lengths and angles of the atoms in the structure, was obtained as a result of molecular optimization. Utilizing the B3LYP/6-31G and B3LYP//SDD techniques, the difference (E) between the HOMO and LUMO energy levels of the the EMPT compound was computed. Using the Mulliken charge distribution method, information was collected about the charge distribution of atoms and different properties of molecular structures. Additionally, DFT/B3LYP/6-31G and DFT/B3LYP//SDD basis of the compound were used to create the MEP map. The atoms surrounding the region were determined to be methyl and hydrogen atoms. These properties have given us information about the parts of the chemical where non-covalent interactions can occur. The grade and charge deploy of the optimized chemical construction were ascertained by means of NBO analysis. For the molecular compound (E), the highest stabilization energy value is 22, respectively 3-phenylthiazolidin, 5-((Z)-4-methylbenzylidene, 2-((E)-4-methylbenzylidene)hydrazineyilidene). The results were 22.96, and 22.40 Kcal/mol. The NLO study stated that the molecule had powerful optical characteristics in a range of orientations. By utilize the B3LYP/6 311G(d,p) method and the B3LYP/SDD method, the compound's isotropic polarizability was determined to be $3.54x10^{-30}$ esu and $3.47x10^{-30}$ esu, respectively. According to the molecular docking simulation of the molecule, it has a high capability to combine with PDB: 5FGK and PDB: 5HBE proteins. The study determined that the binding affinity shift scores for PDB: 5FGK and PDB: 5HBE were, respectively, -7.10 and -6.11 cal/mol. PDB: The 5FGK receptor binding score was found to be more effective. Furthermore, the phthalonitrile group's particular compounds and color regions were subjected to ADME analysis, which produced positive results for ADME analysis in accordance with Lipinski's guidelines.

Conflict of Interest Statement

There is no conflict of interest between the authors.

Statement of Research and Publication Ethics

The study is complied with research and publication ethics.

References

[1] A.-R. L. H. Ismail, N. M. Ismael, and M. Abu-Dief, "Co (II) and Cd (II) complexes based on a tetradentate ONNO donor Schiff base ligand," *DFT calculations and biological studies of Mn (II), Fe (II)*, vol. 1134, pp. 851–862, 2017.

[2] M. Salihović *et al.*, "Synthesis, characterization, antimicrobial activity and DFT study of some novel Schiff bases," *J. Mol. Struct.*, vol. 1241, no. 130670, p. 130670, 2021.

[3] L. Touafri, A. Hellal, S. Chafaa, A. Khelifa, and A. Kadri, "Synthesis, characterisation and DFT studies of three Schiff bases derived from histamine," *J. Mol. Struct.*, vol. 1149, pp. 750–760, 2017.

[4] E. Ermiş, "Synthesis, spectroscopic characterization and DFT calculations of novel Schiff base containing thiophene ring," *J. Mol. Struct.*, vol. 1156, pp. 91–104, 2018.

[5] R. M. Issa, M. K. Awad, and F. M. Atlam, "DFT theoretical studies of antipyrine Schiff bases as corrosion inhibitors: Schiff bases as corrosion inhibitors," *Mater. Corros*, vol. 61, no. 8, pp. 709–714, 2010.

[6] T. Bensafi, "Synthesis, characterization and DFT calculations of linear and NLO properties of novel (Z)-5-benzylidene-3-N (4-methylphenyl)-2-thioxothiazolidin-4-one," *Journal of Sulfur Chemistry*, vol. 42, no. 6, pp. 645–663, 2021.

[7] M. Rashid, J. Yaqoob, N. Khalil, R. Jamil, M. U. Khan, and M. A. Gilani, "Nonlinear optical (NLO) response of boron phosphide nanosheet by alkali metals doping: A DFT study," *Mater. Sci. Semicond. Process.*, vol. 151, no. 107007, p. 107007, 2022.

[8] M. Ishaq, R. A. Shehzad, M. Yaseen, S. Iqbal, K. Ayub, and J. Iqbal, "DFT study of superhalogen-doped borophene with enhanced nonlinear optical properties," *J. Mol. Model.*, vol. 27, no. 6, p. 188, 2021.

[9] T. Michael, J. Frisch, G.W, Bernhard. Schlegel, Gustavo. Scuseria, 2016.

[10] M. Bağlan, "Theoretical Investigation of 1H and 13C NMR Spectra of Diethanol Amine Dithiocarbamate RAFT Agent," *Journal of the Institute of Science and Technology*, vol. 12, no. 3, pp. 1677–1689, 2022.

[11] A. Voityuk Institució Catalana de Recerca i Estudis Avançats (ICREA), Passeig de Lluís Companys, 23, 08010 Barcelona, Spain. alexander. voityuk@gmail. com, A. J. Stasyuk, and S. F. Vyboishchikov, "A simple model for calculating atomic charges in molecules," *Phys. Chem. Chem. Phys.*, vol. 20, no. 36, pp. 23328–23337, 2018.

[12] P. Bultinck *et al.*, "The electronegativity equalization method II: Applicability of different atomic charge schemes," *J. Phys. Chem. A*, vol. 106, no. 34, pp. 7895–7901, 2002.

[13] M. Bağlan, K. Gören, and Ü. Yildiko, "HOMO–LUMO, NBO, NLO, MEP analysis and molecular docking using DFT calculations in DFPA molecule," *Int. J. Chem. Technol.*, pp. 208–217, 2023.

[14] V. Choudhary, A. Bhatt, D. Dash, and N. Sharma, "DFT calculations on molecular structures, HOMO-LUMO study, reactivity descriptors and spectral analyses of newly synthesized diorganotin (IV) 2-chloridophenylacetohydroxamate complexes," J. Comput. Chem., pp. 2354–2363, 2019.

[15] F. Pereira, K. Xiao, D. A. R. S. Latino, C. Wu, Q. Zhang, and J. Aires-de-Sousa, "Machine learning methods to predict density functional theory B3LYP energies of HOMO and LUMO orbitals," *J. Chem. Inf. Model.*, vol. 57, no. 1, pp. 11–21, 2017.

[16] E. S. Marinho and M. M. Marinho, "A DFT study of synthetic drug topiroxostat: MEP, HOMO, LUMO," *Int. J. Sci. Eng. Res*, vol. 7, no. 8, 2016.

[17] S. Chandrasekar, V. Balachandran, and H.-S. Evans, "Synthesis, crystal structures HOMO-LUMO analysis and DFT calculation of new complexes of p-substituted dibenzyltin chlorides and 1, 10-phenanthroline," *Spectrochimica Acta Part A: Molecular and Biomolecular Spectroscopy*, vol. 143, pp. 136–146, 2015.

[18] V. Balachandran, G. Mahalakshmi, A. Lakshmi, and A. Janaki, "DFT, FT-Raman, FT-IR, HOMO-LUMO and NBO studies of 4-Methylmorpholine," *Spectrochim. Acta A Mol. Biomol. Spectrosc.*, vol. 97, pp. 1101–1110, 2012.

[19] Ü. Yildiko and G. K. Dft, "DFT Calculatıons and Molecular Dockıng Study ın 6-(2"-pyrrolıdınone-5"-Yl)-(," *Epıcatechın Molecule From Flavonoıds. Eskişehir Teknik Üniversitesi Bilim ve Teknoloji Dergisi B-Teorik Bilimler*, vol. 11, pp. 43–55, 2023.

[20] S. Guidara and H. Feki, "Structural, vibrational, NLO, MEP, NBO analysis and DFT calculation of bis 2, 5-dimethylanilinium sulfate," *Journal of Molecular Structure*, vol. 1080, pp. 176–187, 2015.

[21] B. K. Shukla, "DFT calculations on molecular structure, MEP and HOMO-LUMO study of 3-phenyl-1-(methyl-sulfonyl)-1H-pyrazolo pyrimidine-4-amine," *Materials Today: Proceedings*, vol. 49, pp. 3056–3060, 2022.

[22] N. Uludağ, G. Serdaroğlu, Ir, and N. Uv-Vis, "An improved synthesis, spectroscopic (FT-IR, NMR) study and DFT computational analysis (IR, NMR, UV-Vis, MEP diagrams, NBO, NLO, FMO) of the 1, 5-methanoazocino indole core structure," *Journal of Molecular Structure*, vol. 1155, pp. 548–560, 2018.

[23] S. Sevvanthi, "MEP) studies and molecular docking on benzodiazepine derivatives-heterocyclic organic arenes," *Chemical Data Collections*, vol. 30, 2020.

[24] Ü. Yildiko, "Computational Investigation of 5.5'', 7''-trihydroxy-3, 7-dimethoxy-4'-4'''-O-biflavone from Flavonoids Using DFT Calculations and Molecular Docking," *Adıyaman University Journal of Science*, vol. 12, no. 2, pp. 283–298, 2022.

[25] R. Saravanan, S. Seshadri, S. Gunasekaran, and R. Mendoza-Meroño, "Crystallographic, experimental (FT-IR and FT-RS) and theoretical (DFT) investigation, UV-Vis, MEP, HOMO-LUMO and NBO/NLMO of (E)-1-[1-(4-Chlorophenyl) ethylidene] thiosemicarbazide," *Spectrochimica Acta Part A: Molecular and Biomolecular Spectroscopy*, vol. 121, pp. 268–275, 2014.

[26] K. Gören, "DFT Computations and Molecular Docking Studies of 3-(6-(3-aminophenyl) thiazolo [1, 2, 4] triazol-2-yl)-2H-chromen-2-one (ATTC) Molecule," *Hittite Journal of Science and Engineering*, vol. 10, no. 1, pp. 11–19, 2023.

[27] S. Sundaram, V. N. Vijayakumar, and V. Balasubramanian, "Electronic and structure conformational analysis (HOMO-LUMO, MEP, NBO, ELF, LOL, AIM) of hydrogen bond binary liquid crystal mixture: DFT/TD-DFT approach," *Comput. Theor. Chem.*, vol. 1217, no. 113920, p. 113920, 2022.

[28] M. Khattab and A. A. Al-Karmalawy, "Revisiting activity of some Nocodazole analogues as a potential anticancer drugs using molecular docking and DFT calculations," *Front. Chem.*, vol. 9, p. 628398, 2021.

[29] N. A. Dlala, Y. Bouazizi, H. Ghalla, and N. Hamdi, "DFT calculations and molecular docking studies on a chromene derivative," *J. Chem.*, vol. 2021, pp. 1–17, 2021.

[30] V. K. Singh *et al.*, "Docking, ADMET prediction, DFT analysis, synthesis, cytotoxicity, antibacterial screening and QSAR analysis of diarylpyrimidine derivatives," *J. Mol. Struct.*, vol. 1247, no. 131400, p. 131400, 2022.

[31] C. A. Lipinski, "Lead-and drug-like compounds: the rule-of-five revolution," *Drug discovery today: Technologies*, vol. 1, no. 4, pp. 337–341, 2004.

[32] A.-S. Badran and M. A. Ibrahim, "Synthesis, spectral characterization, DFT and in silico ADME studies of the novel pyrido[1,2-a]benzimidazoles and pyrazolo[3,4-b]pyridines," *J. Mol. Struct.*, vol. 1274, no. 134454, p. 134454, 2023.